Flow hydrodynamics drive effective fish attraction behaviour into slotted fishway entrances

Maryam Farzadkhoo (maryam.farzadkhoo@unsw.edu.au)
University of New South Wales https://orcid.org/0000-0003-1651-5706
Richard T Kingsford
University of New South Wales
Iain M. Suthers
University of New South Wales
Stefan Felder
University of New South Wales

Research Article

Keywords: Attraction jet flow, fish behaviour, fish swimming trajectories, TKE, Australian native fish

Posted Date: April 3rd, 2023

DOI: https://doi.org/10.21203/rs.3.rs-2700500/v1

Version of Record: A version of this preprint was published at Journal of Hydrodynamics on September 12th, 2023. See the published version at https://doi.org/10.1007/s42241-023-0047-6.

Abstract

Effective fishways rely on attracting fish, utilising the natural rheotactic behaviour of fish to orient into an attraction flow near the entrance. Despite the critical importance of attraction, understanding of the hydrodynamics of vertical slot entrances in relation to fish behaviour remains poor. Herein, hydrodynamic measurements of flows at slotted fishway entrances were experimented with two different designs, two velocities, three water depths, and two fish species, silver perch (*Bidyanus bidyanus*) and Australian bass (*Percalates novemaculeata*). Fish behaviours were tracked in relation to hydrodynamic measures of three-dimensional velocity and turbulent kinetic energy (*TKE*). There were distinct differences in the attraction flow between entrance designs, irrespective of velocity and water depth. Plain slotted entrance produced a more symmetric flow in the centre of the flume, causing fish to approach the entrance by skirting the core of the attraction jet flow and areas of high turbulence. In contrast, streamlined slotted entrance design resulted in an asymmetric attraction flow which guided fish along the wall of the flume, improving attraction for both species. There were clear patterns in swimming trajectories for silver perch, swimming along the sidewalls of the observation zone towards the entrance, but Australian bass were less predictable, using random routes on their way to the slotted entrance. Both species preferred areas of low turbulence ($TKE < 0.02$ m^2/s^2) and the asymmetric attraction flow along one of the sidewalls created by the streamlined entrance improved the fish attraction. This work has important implications for design of vertical slotted entrance systems.

1 Introduction

Dams, weirs and levees are important for flood protection, hydropower generation, and for water supply [1] but contribute to significantly reduced fish migration and fish population diversity in rivers and estuaries [2, 3]. Fishways mitigate this problem, enabling fish movement past barriers [4]. Most constructed fishways, such as vertical slot and pool fishways, use sloped open channels divided by cross-walls into a series of pools to allow fish to swim past a barrier [5, 6]. Other fishway types transport fish through closed conduit system of pipes such as the Whooshh system [7] and the Tube Fishway [8–10]

Most fishways rely on the natural rheotactic behaviour of fish to attract them into a fishway entrance, before they move past a barrier. Rheotaxis orientates fish into a current using the sensory cells of the fish's lateral line system [11]. Therefore, fish movement depends on fishway design (e.g., pool dimension and slot design), channel slope [12], and associated flow conditions (e.g. water depths, velocities and turbulence). Turbulence can affect fish swimming capacity, reducing fish swimming speed and stability [13–15]. Inadequate attraction flow can reduce overall fishway effectiveness [16, 17], and may delay fish attraction which increases predation risk [18]. It is clear that improved understanding of relationships between fish behaviour and the hydrodynamics of attraction flows could significantly improve fishway performance [18–22]. Complicating this relationship, behaviour of different fish species also varies, reflecting differences in swimming speeds, swimming path selection, and response to turbulent flows [21].

Despite this importance, there is currently little documented understanding on suitable flow hydrodynamics for effective fish attraction [23], particularly in relation to velocity and turbulence. Velocity of attraction flows needs to be sufficient to induce fish rheotaxis and swimming through the fishway entrance, but not too high to affect swimming ability [17, 24]. Salmonids are attracted by up to 10% of the main river discharge into fishways [25–27]. Attraction flow velocities of more than 2 m/s are recommended for economically significant salmonid fish species, such as Pacific lamprey (*Lampetra tridentata*), American shad (*Alosa sapidissima*), and Pacific salmon (*Oncorhynchus*) [28, 29]. However, such velocities exceed the recommended swimming capabilities of some non-salmonoid species: 0.4 m/s for Prenant's schizothoracin (*Schizothorax prenanti*) [30]; 0.25 m/s for Iberian barbel (*Luciobarbus bocagei*) [31]; and 0.2 m/s to 0.3 m/s for perch barbel (*Percocypris pingi*) and grass carp (*Ctenopharyngodon idella*) respectively [23, 32]. Juvenile silver perch (*Bidyanus bidyanus*) and Australian bass (*Percalates novemaculeata*) had preferred attraction flow velocity of 0.15 m/s [33, 34].

TKE is most commonly used hydrodynamic descriptor for fish attraction into fishways [12, 35], measuring mean kinetic energy associated with velocity fluctuations [36]. Fishway entrances, designed for salmonoids, operate with *TKE* values of 0.1–1.2 m^2/s^2 [37–40], possibly too high for non-salmonid species with lower swimming capabilities [41]. [24] investigated attraction flows for six endemic fishes in China showing that $0 < TKE < 0.02$ m^2/s^2 allowed fish attraction. Similarly, bighead carp (*Hypophthalmichthys nobilis*) and grass carp (*Ctenopharyngodon idella*) were best attracted into a vertical slot fishway for $TKE < 0.02$ m^2/s^2 [42], while 0.002 $m^2/s^2 < TKE < 0.003$ m^2/s^2 allowed optimal attraction of three socio-economical important fish species in the Jing River in China (*Cyprinidae Phoxinus lagowskii*, *Opsariichthys bidens*, and *cobitidae Triplophysa stoliczkae*) in an entrance channel with a sluice gate [43].

In this study, the relationships between hydrodynamics of the attraction flow and fish behaviour were investigated in two different vertical slotted entrance designs (plain and streamlined) for different velocities and water depths for two fish species (silver perch and Australian bass). Firstly, the visual observations of the flow patterns of the attraction flows as well as detailed measurements of the velocity field were reported upstream and downstream of the slotted entrance. Secondly, the fish attraction behaviour in relation to the attraction flows were examined for the two slotted entrance designs as well as the range of velocities V_a and water depth d to improve attraction of fish to vertical slotted fishway entrances.

2 Material And Methods

2.1 Experiments

Experiments were conducted at the UNSW Water Research Laboratory in an open-channel flume with glass sidewalls of 6 m length, 0.6 m width, and 0.6 m height. The flume had a 1.1 m long observation channel (*OC*), with a slotted entrance (*SE*) of 0.03 m width at the upstream end. Fish were attracted into a pipe T-section, called transfer chamber (*TC*) as used in Tube Fishways [8] (Fig. 1a). The pipe T-section

had an inlet pipe of 0.05 m diameter on the upstream side which expanded gradually towards the T-section (Fig. 1a). The T-section of the transfer chamber was open at the top to provide similar light conditions as in the observation channel. Flow direction was through the transfer chamber and into the observation channel (Fig. 1), reflecting placement of a fishway in a river.

Experiments were conducted for three water depths (d) at the slotted entrance (Fig. 1), 0.08 m, 0.18 m, and 0.32 m, respectively corresponding to transfer chamber diameters D_a = 0.1 m, 0.225 m and 0.4 m and lengths L_a = 0.25 m, 0.6 m, and 1 m, such that the ratio of water depth to the transfer chamber diameter was 80% (d/D_a = 0.8), ensuring open channel flows inside the transfer chamber. The water depths were controlled by adjusting a weir at the downstream end of the observation channel (Fig. 1a). Experiments were conducted for a range of attraction flows: $0 \leq Q \leq 4.8$ L/s, producing three different attraction velocities at the slotted entrance: V_a = 0 m/s, 0.15 m/s, and 0.5 m/s (Table 1). Using a recirculation system, flows were pumped through an inlet pipe into the transfer chamber, before passing through the slotted entrance into the observation channel (Fig. 1a). The resulting attraction flow emerged as jet (hereafter referred to as a jet flow), designed to attract fish. Flow was measured with a Yamatake Honeywell flowmeter (accuracy of ± 0.5% of the flow rate). Water flowed from the observation channel via gravity into a ground reservoir before being pumped to a 6 m^3 large recirculation reservoir. Experiments used either a plain entrance design (as the most common entrance for vertical slot fishways) (Fig. 1b, Table 1), or a streamlined entrance design with two 45° angled sidewalls next to the slotted entrance (which was previously proved to improve attraction for silver perch and Australian bass [33] (Fig. 1c, Table 1).

Table 1
Summary of experimental flow conditions, water depth (d), transfer chamber diameter (D_a), attraction flow (Q), attraction flow velocity at the slotted entrance (V_a), the corresponding cross-sectional average velocity in the transfer chamber (V_{TC}), the Froude number at the slotted entrance $Fr_s = \mathrm{V_a}/\sqrt{\mathrm{gd}}$, the Reynolds number at the slotted entrance $\mathrm{Re_s} = \rho\ \mathrm{V_a d}/\mu$(where ρ is the water density and μ is the dynamic viscosity of water), and the momentum flux at the slot $\mathrm{M} = \rho\ \mathrm{Q}\ \mathrm{V_a}$ [44]. (See Fig. 1 for details on the two slotted entrance designs)

d (m)	D_a (m)	*Q* (l/s)	V_a (m/s)	V_{TC} (m/s)	Fr_s (-)	Re_s (-)	*M* (N)	Slotted entrance
0.08	0.1	0	0	0	0	0	0	Plain
0.08	0.1	0.36	0.15	0.06	0.16	1.19×10^4	0.05	Plain/ streamlined
0.08	0.1	1.20	0.50	0.19	0.56	3.19×10^4	0.59	plain
0.18	0.225	0	0	0	0	0	0	Plain
0.18	0.225	0.81	0.15	0.03	0.11	2.69×10^4	0.12	Plain/ streamlined
0.18	0.225	2.70	0.50	0.08	0.37	8.97×10^4	1.34	Plain
0.32	0.4	0	0	0	0	0	0	Plain
0.32	0.4	1.44	0.15	0.01	0.08	4.78×10^4	0.21	Plain/ streamlined
0.32	0.4	4.80	0.50	0.05	0.28	1.59×10^5	2.39	Plain

2.2 Hydrodynamic measurements

Measurements of the hydrodynamic flow properties were conducted with a SonTek 16 MHz Micro Acoustic Doppler Velocimeter (ADV). Velocities were measured across a grid of 80 points in the observation channel, with focus on the attraction jet flow region, just downstream of the slotted entrance and at 19 measurement points inside the transfer chamber (Figs. S1 in Supplementary Material). The ADV recorded instantaneous velocities in three directions (v_x, v_y, and v_Z, Fig. 1), with a sampling frequency of 200 Hz and for four minutes at each measurement point. Velocity sampling duration was the convergence of mean and standard deviation, identified using sensitivity analysis at three representative locations: just downstream of the slotted entrance (X = 0.05 m), in the middle of the observation chamber (X = 0.55), and close to the weir (X = 1.05 m) (Fig. 1). The measurements were taken

in three horizontal planes at depths of $Z = 0.1\ d$, $0.3\ d$, and $0.5\ d$ for $d = 0.18$ m and at one horizontal plane of $Z = 0.3\ d$ for $d = 0.08$ m and 0.32 m, respectively. These depths represented fish preferences in entering the lower half of the slotted entrance [33]. In total, 1500 measurement points were taken for all the combinations of d, V_a, and slotted entrance design in this study. Vertical profiles of velocities were also measured at three locations downstream of the slotted entrance ($X = 0.05$ m, 0.1 m, and 0.2 m) for $d = 0.18$ m and 0.32 m to check variability of velocity with depth. To improve the raw data quality of the ADV, clay powder was added before ADV measurements in order to seed the water. Win-ADV was used to filter the raw data removing low quality data, with a signal-to-noise ratio below 5 dB and a correlation coefficient below 70%, followed by application of the despiking filter [45, 46]. The resulting velocity time series was post-processed, yielding mean velocities V_x, V_y, V_z in x, y and z directions at each measurement point, their corresponding standard deviations (v_x', v_y' and v_z'), and turbulent kinetic energy TKE [36]:

$$\mathrm{TTKE} = 0.5\ \left[\overline{\left(\mathrm{v_x}'\right)^2} + \overline{\left(\mathrm{v_y}'\right)^2}\ + \overline{\left(\mathrm{v_z}'\right)^2}\right]$$

1

To visualize the flow patterns of the attraction flows downstream of the entrance, experiments with blue dye complemented the quantitative ADV measurements. High-concentration dye was injected through a stainless-steel nozzle into the flow at the slotted entrance at a water depth of $Z \sim 0.5\ d$ for all experiments. The dye cloud motion was recorded with two GoPro (HERO8 black edition) video cameras (1080p, 60 fps), from top view and through the sidewall visualizing the attraction flow patterns.

2.3 Fish behaviour

Silver perch (total length, TL = 67–87 mm) and Australian bass (TL = 117–152 mm) were maintained in 0.14 m^3 or 0.20 m^3 tanks at the UNSW Water Research Laboratory [33]. In that study, seven replicates with groups of five silver perch and five replicates with groups of five Australian bass were conducted for one hour for all the combinations of $d = 0.08$ m, 0.18 m, and 0.32 m, V_a = 0 m/s, 0.15 m/s, and 0.5 m/s, and slotted entrance design (plain and streamlined). A total of 136 trials showed that fish could be attracted irrespective of the water depth and attraction flow velocity with $d = 0.18$ m and the streamlined entrance with V_a = 0.15 m/s representing the most successful attraction flow conditions [33].

In the present study, top and side view recordings were manually re-analysed to record the pre-entry fish locations at the vicinity of the slotted entrance (see yellow and green shaded areas in Fig. 1a) every second during the 1-hour filming of each observation trial on a fine-scale grid: n_{NJ-L} (non-jet-left), n_{NJ-R} (non-jet-right) and n_{J-C} (jet-centre) corresponding to the number of fish entries from left, right, and centre of the attraction flow. For the streamlined entrance, the attraction jet was deflected towards one of the sidewalls downstream of the slotted entrance, and the regions for the pre-entry fish locations were divided into the centre, the jet region on one side and a non-jet region on the other side. For easier readability, the

jet is shown on the left sidewall of the streamlined entrance, while the jets were also observed on the opposing side.

Locations of fish before they entered the entrance (pre-entry) were modelled using linear models (LMs) and ANOVA to identify the relative importance of predictors (attraction direction, velocity, and water depth) for both species. To meet assumptions of normality, a log transformation was required. For a significant interactive effect, the Estimated Marginal Means package was used for contrast analysis to identify specific differences [47]. All statistical analysis were performed using the R software (1.1.456; R Core Team, 2021). Statistical significance was at $P < 0.05$.

In addition, videos of the swimming trajectories of 60 fish (30 silver perch and 30 Australian bass) of the first fish entries (frame by frame, 60 fps) across the observation channel were analysed, using open-source video analysis software Tracker [48]. The time series of the resulting coordinates of the fish swimming trajectories in the *x-y* plane were plotted across the observation channel. The trajectory analysis focussed on $d = 0.18$ m for the plain entrance with $V_a = 0$ m/s and 0.15 m/s and the streamlined entrance for $V_a = 0.15$ m/s for both fish species. To confirm the strong preference of fish to swim along the jet trajectory for the streamlined entrance, additional analysis of the approach swimming trajectories of 45 silver perch and 45 Australian bass for first fish entries with the streamlined entrance ($V_a = 0.15$) were conducted for all water depths ($d = 0.08$, 0.18, 0.32 m). The fish swimming trajectories were divided into two distinct areas of jet and non-jet regions upstream of the slotted entrance.

3 Results: Hydrodynamics Of Attraction Flows

This section presents representative results of the flow pattern observations and quantitative hydrodynamic measurements for plain and streamlined entrances, supported by comprehensive results (Figs. S2-S5 in Supplementary Material).

3.1 Plain entrance

Generally, there were clear flow patterns for the plain slotted entrance, with a jet flow emerging out of the slotted entrance, gradually expanding in downstream direction and eventually dispersing (Fig. 2). The overall jet patterns were consistent with free jets in open channel flows [49, 50] (Fig. 2). Downstream of the entrance, the main jet trajectory diverged towards one side of the observation channel (indicated by solid lines, grey and black in Fig. 2a and the blue dye in Figs. 2b-c), creating a recirculation pattern in the observation channel (dashed lines in Fig. 2a). Depending on the water depth and the attraction velocity, a second recirculation zone was maintained in the corner, next to where the main jet first emerged (Figs. 2a-b).

Figure 3 shows typical results of the streamwise velocities. The velocities were normalised with V_a and the same colour scheme was used for all flow conditions to enable comparison between flow conditions

(Fig. 3). The maximum normalised streamwise velocity ($1.15 < V_x / V_a < 1.3$) occurred just downstream of the slot, in centreline, and the jet decayed rapidly along the jet ($0.2 < V_x / V_a < 0.8$), confirming the overall flow pattern observations (Fig. 2). The velocity decay was consistent with those observed for single vertical slot pools (Liu et al. 2006). Further downstream, the jet propagated along one of the sidewalls initiating recirculation motions ($-0.6 < V_x / V_a < 0.2$), which was consistent with the observations of [51]. A smaller recirculation zone with very low velocities occurred in the corner, adjacent to the main jet (Fig. 3). While the overall velocity distributions were consistent, irrespective of d (Fig. 3 and Fig. S2 in Supplementary Material), the jet for $d = 0.18$ m tended to travel downstream in a straighter direction compared with other two water depths (Fig. S2 in Supplementary Material), creating two more equal recirculation zones on either side of the jet. This is also reflected in the transverse velocity distributions, with recirculation motions of almost similar size, on either side of the jet for $d = 0.18$ m, but differently sized for $d = 0.08$ m and 0.32 m (Fig. S2 in Supplementary Material).

A comparison of velocities across different horizontal layers (Z) for $d = 0.18$ m, showed higher V_x / V_a and V_z / V_a at $Z = 0.1\ d$ just downstream of the slotted entrance compared to $Z = 0.3\ d$ and $0.5\ d$ (Fig. S3 in Supplementary Material), suggesting that the jet had high velocities closer to the bottom. There was a similar variation in the vertical profiles of velocities at three points along the observation channel ($X =$ 0.05 m, 0.1 m, and 0.2 m downstream of the slotted entrance) across water depths. Increasing the attraction flow from $V_a = 0.15$ m/s to 0.5 m/s had little impact on the streamwise, transverse, and vertical velocity distributions in the observation channel for the respective water depth (Fig. S2 in Supplementary Material).

Inside the transfer chamber, the flows were more complex, compared to the observation channel (Figs. 3a-d, Fig. S2 in Supplementary Material). There were two velocity regions: one with higher velocity ($0.2 < V_x / V_a < 1.3$) and one with lower/negative velocity (reverse flow) ($-0.6 < V_x / V_a < 0.2$), irrespective of V_a and d. Increasing the water depth from $d = 0.08$ m to $d = 0.32$ m reduced the magnitude and the extent of V_z / V_a inside the transfer chamber. There was also a strong change in magnitude of streamwise and vertical velocity components across the water depth for $d = 0.18$ m (Fig. S3 in Supplementary Material), suggesting a highly three-dimensional flow inside the transfer chamber.

Typically, the strongest dimensionless turbulent kinetic energy ($\sqrt{\mathrm{TKE}} / V_a$) was just downstream of the slot, decaying in value and widening along the jet (Fig. 4; Fig. S2 in Supplementary Material). The values of $\sqrt{\mathrm{TKE}} / V_a$ in this region were similar for all flow conditions and water depths, indicating similar jet flow properties irrespective of water depth (Fig. S2 in Supplementary Material). Turbulent kinetic energy decayed along the jet, consistent with the observations of the velocities. In the remaining part of the observation channel (the blue zone in Fig. 4), $\sqrt{\mathrm{TKE}} / V_a$ values were much lower ($\sqrt{\mathrm{TKE}} / V_a < 0.3$; $TKE < 0.002$ m^2/s^2 for $V_a = 0.15$ m/s and $TKE < 0.02$ m^2/s^2 for $V_a = 0.5$ m/s) than the main jet trajectory, consistent with observations of reductions in flow velocity away from the attraction jet.

Magnitudes of $\sqrt{\mathrm{TKE}}$ / V_a varied across different horizontal layers (Fig. S3 in Supplementary Material). For example, for d = 0.18 m at Z = 0.1 d, TKE = 0.1 m^2/s^2 ($\sqrt{\mathrm{TKE}}$ = 0.70 V_a) for V_a = 0.5 m/s while TKE reduced to TKE = 0.05 m^2/s^2 ($\sqrt{\mathrm{TKE}}$ = 0.44 V_a) at Z = 0.5 d (Fig. S3 in Supplementary Material). This was consistent with variation in velocities across the attraction flow depth, indicating strong three-dimensionality in the attraction jet. For a given d and V_a, TKE values were relatively higher inside the transfer chamber compared to those in the observation channel (Fig. S2 in Supplementary Material). Irrespective of the water depth, increasing the attraction flow velocity from V_a = 0.15 m/s to 0.5 m/s resulted in more than doubled $\sqrt{\mathrm{TKE}}/V_a$ inside the transfer chamber (Fig. 4; Fig. S2 in Supplementary Material). Similarly, $\sqrt{\mathrm{TKE}}/V_a$ inside the transfer chamber differed across different horizontal layers for d = 0.18 m, consistent with velocity observations (Fig. S3 in Supplementary Material).

3.2 Streamlined entrance

For the streamlined entrance, there was a distinct pattern of the attraction jet clinging to one of the two 45º angled sidewalls, immediately downstream of the slotted entrance (Fig. 5). Irrespective of the water depth, the jet followed the sidewall, initiating a steady recirculation motion across the observation channel. This jet deflection was probably caused by the angled walls initiating a “Coanda effect”, in which a jet flow deflects from a straight direction by a nearby wall [52, 53].

The distinctive jet deflection to one side and recirculation motion were reflected in the velocity distributions in the observation channel, irrespective of flow conditions (Fig. 6; Fig. S4 in Supplementary Material). Comparison of the velocity distributions for different d, showed consistent maximum streamwise velocities just downstream of the slotted entrance (Figs. 6a-b; Fig. S4 in Supplementary Material). The jet extended across a wider area of the observation channel when d was smaller (with magnitudes of 0.2 < V_x / V_a < 1.8) (Figs. 6a-b; Fig. S4 in Supplementary Material). Across the three horizontal planes (Z = 0.1 d, 0.3 d, 0.5 d) for d = 0.18 m, velocity varied with depth. It was highest near the bottom (Z = 0.1 d) (Figs. 6c-d; Fig. S5 in Supplementary Material). The velocity decay along the deflected jet occurred faster compared to the streamlined entrance, which is likely linked to the Coanda effect which slows the velocity much more than a free jet [53] (Fig. A1, Appendix). Inside the transfer chamber, velocities varied strongly as well (Figs. 6c-d; Fig. S5 in Supplementary Material). The flows inside the transfer chamber were characterised by a strong velocity gradient and a recirculation motion (Fig. 6; Fig. S4 in Supplementary Material).

Normalised turbulent kinetic energy, $\sqrt{\mathrm{TKE}}/V_a$, was high along the attraction jet trajectory and close to an angled sidewall (Fig. 7). With increasing water depth, strong turbulent kinetic energy ($\sqrt{\mathrm{TKE}}/V_a$ > 0.6; TKE >0.008 m^2/s^2) extended across a large area of the observation channel, probably linked to strong momentum flux (Fig. S4 in Supplementary Material). The magnitude of $\sqrt{\mathrm{TKE}}$ / V_a increased near the bottom (Z = 0.1 d) for d = 0.18 m (Fig. S5 in Supplementary Material). Inside the transfer

chamber, *TKE* varied (0.005 m^2/s^2 < *TKE* < 0.02 m^2/s^2) reflecting the complex 3-D flow patterns (Fig. 7; Fig. S4 in Supplementary Material).

4 Results: Fish Response To Attraction Flow

In this section, the pre-entry fish locations at the vicinity of the slotted entrance are compared with the attraction jet flow patterns (Section 4.1) and the fish swimming trajectories are compared with the distributions of turbulent kinetic energy (Section 4.2) providing guidance on the interaction of fish behaviour with attraction flow hydrodynamics.

4.1 Pre-entry location

The distribution of locations of silver perch and Australian bass before they entered (pre-entry locations) the two slotted entrance designs varied with flow conditions (Fig. 8). Statistical analysis showed complex 3-way interactions among the attraction direction taken by fish and different velocity and water depth, which was significant ($P = 0.001$, $F_{6,66} = 4.06$) for silver perch (Table A1, Appendix), albeit not significant ($P = 0.96$, $F_{3,60} = 0.09$) for Australian bass (Table A2, Appendix). There were also significant 2-way interactions between the attraction direction and velocity ($P < 0.001$) for both species (Table A1-A2, Appendix), revealing that pre-entry locations varied with velocities and entrance designs. Overall, most fish entered from the jet region of the streamlined entrance, irrespective of the water depth (T ratio = 9.40, $P < 0.001$ for silver perch, Table A3, Appendix; T ratio = 5.24, $P < 0.001$ for Australian bass, Table A4, Appendix). Contrastingly, there was no significant tendency for silver perch or Australian bass to enter via jet-region for plain entrance (T ratio = − 0.4, $P = 0.63$ for silver perch; T ratio = − 1.17, $P = 0.24$ for Australian bass). When considering the attraction direction in the vicinity of the streamlined entrance, more than 80% of fish entries occurred via the jet with only a small fraction attracted through the centre and the non-jet side, irrespective of the fish species and the water depth (dark green colour in Fig. 8). For the plain entrance with a centre jet just downstream of the slotted entrance, the number of pre-entry locations for the silver perch and Australian bass were similar among the three entry categories, with a slight dominance for the entry at the jet-centre for $V_a = 0.15$ m/s for all water depths (orange colour in Fig. 8). For the condition with no attraction velocity ($V_a = 0$ m/s), the results were similar with a balanced re-entry location. However, for the largest attraction flow velocity ($V_a = 0.5$ m/s), there was a tendency for fish entry via the jet-centre for both fish species and most water depths (Fig. 8).

4.2 Fish swimming trajectories

There were clear patterns in swimming trajectories for silver perch, but Australian bass used varied swimming paths for different slotted entrance design (Fig. 9). Silver perch tended to swim along the sidewalls and corners with no preference for any specific side, for the plain entrance and the control flow condition ($V_a = 0$ m/s) (Fig. 9a), while Australian bass selected more direct paths within the centre part of

the observation channel (Fig. 9b). When an attraction velocity was present (V_a = 0.15 m/s), most silver perch swam along the sidewall where there were slightly higher values of *TKE*, i.e. *TKE* ≈ 0.0005 m^2/s^2, next to the sidewall, compared to *TKE* ≈ 0.0002 m^2/s^2 on the opposite sidewall (Fig. 9c). It appeared that silver perch responded to the slightly higher *TKE* values indicating that small changes in hydrodynamic flow conditions can have a large effect on the fish swimming trajectory. Along their trajectory, silver perch preferably passed through the recirculation zone in the corner and avoided to swim along the main jet flow with $0.35 < \sqrt{\mathrm{TKE}} / V_a < 0.6$ (0.002 m^2/s^2 < *TKE* < 0.008 m^2/s^2) (Fig. 9c). They then entered the transfer chamber by swimming towards the jet and making a 90° turn into the slotted entrance (Fig. 9c). Australian bass used more varied routes, with a slight preference for areas with higher *TKE* values in the observation channel (Fig. 9d). Also, their trajectories were similar to the no-flow control condition (Figs. 9b and d). One Australian bass followed the edge of the main jet (0.002 m^2/s^2 < *TKE* < 0.008 m^2/s^2), while another bass crossed through the jet region towards the slotted entrance (Fig. 9d).

The observation for the streamlined slotted entrance were substantially different for both fish species. Most silver perch and Australian bass followed the main trajectory of the jet with regions of maximum *TKE* (Figs. 9e-f). Both species swam along the jet path with the highest *TKE* values in the observation channel ($0.2 < \sqrt{\mathrm{TKE}} / V_a < 0.6$; 0.001 m^2/s^2 < *TKE* < 0.008 m^2/s^2). A few fish sought out a path away from the jet, with much lower values of *TKE* ($0 < \sqrt{\mathrm{TKE}} / V_a < 0.2$; 0 m^2/s^2 < *TKE* < 0.001 m^2/s^2), skirting the jet just before heading to the slotted entrance (Fig. 9e-f).

Further, when silver perch approached the streamlined entrance from the far end of the observation channel for V_a = 0.15 m/s, most swam along the jet into the slotted entrance, whatever the water depth (Fig. 10a). This finding was consistent with the more detailed fish swimming trajectory observations for *d* = 0.18 m (Fig. 9e) highlighting that silver perch are strongly responsive to attraction jet flows. In contrast, the observations of Australian bass suggested less Australian bass followed the jet flow trajectory for *d* = 0.08 m and 0.32 m (Fig. 10b).

5 Discussion

There is relatively poor understanding of fish attraction to slotted fish entrances in relation to the flow hydrodynamics. The present results showed how fish behaviour varied between two juvenile Australian fish species and two slotted entrance designs, reflecting on the response of fish to flow hydrodynamics, across a range of water depths and flow velocities. There were strong responses from one of the fish species, juvenile silver perch, while the other species, Australian bass, was less responsive. Importantly, hydrodynamics explained the movements of the fish, providing some novel insights into fish behaviour when attracted to flow, valuable in considering effectiveness of fishways. As expected, flow hydrodynamics was particularly sensitive to the entrance design.

Plain and streamlined entrances generated different jet flows (Figs. 2–7). The plain slotted entrance created a central jet with typical decay in velocity magnitudes and turbulent kinetic energy in downstream

direction, while the streamlined slotted entrance deflected the jets towards a sidewall. The deviation of a jet flow from its original path when it encounters a nearby wall is the "Coanda effect" [52, 53]. The presence of sidewalls causes pressure gradients perpendicular to the jet, deflecting the attraction flow. Additionally, the momentum imbalance generated by the jets, within the transfer chamber, may also have contributed to the deflection of the attraction flows to one side [54]. Most juvenile fish preferred to swim into the main attraction flow irrespective of the water depth, following the distinct jet flow along one of the sidewalls (Figs. 9–10). The interaction of the jet with the sidewall boundary layer likely created optimum attraction conditions of flow for the streamlined entrance as it was more effective for fish than the plain entrance [33]. In streams, fish use the area near structures because they not only provide regions of low flow but also an opportunity to swim more efficiently given the effects of solid walls [55–57]. Wall-like structures are also well-known refuges suitable for fish predator avoidance [55, 58].

For the plain entrance, most silver perch also tended to swim along the sidewalls of the observation zone towards the entrance, but Australian bass were less predictable, moving along different paths, even when there was no flow (Figs. 9b and d). Both fish species generally moved along low-velocity zones, avoiding areas of high turbulence. This reflects fish movements in other rivers, concentrated along reduced velocity areas, minimising energy expenditure [12, 59, 60] and areas of unpredictable turbulence [61]. Fish respond to hydrodynamic processes with rheotactic responses mediated through lateral line organs, vision, and vestibular functions [11, 62], guiding fish with hydraulic signals [43, 63, 64].

TKE is a key factor governing attraction flow hydrodynamics for fish [12, 65]. For both slotted entrances, the attraction jet created areas with varying flow velocities and *TKE* distributions in the observation channel providing diverse attraction flow conditions which allowed our tested fish to freely select attraction paths, probably reflecting body morphology and biology [58]. The successful use of such asymmetric attraction flows occurs in other vertical slot fishways [5, 66–69]. For improved attraction, several parameters need to be considered, including the residence time of fish in the fishway without escaping downstream into the observation channel which is negatively correlated with *TKE* [40, 70]. Manipulating depth and velocity can be critical, with silver perch and Australian bass exhibiting the highest residence time (up to 95%) for d = 0.18 m and V_a = 0.15 m/s compared to other depths and velocities [33]. Based on our analysis, juvenile silver perch and Australian bass moved best when *TKE* < 0.02 m^2/s^2. This is similar to *TKE* values favouring attraction of tropical fish species at vertical slot entrance channels [24, 42, 43]. In our study, *TKE* was significantly higher than 0.2 m^2/s^2 inside the observation channel and the transfer chamber when V_a = 0.5 m/s, irrespective of water depth (d). This probably resulted in fewer fish entrances with significantly lower residence time in the transfer chamber under these flow conditions [33], beyond the fish swimming capability [8, 71, 72].

This study provided important guidance to optimise fish attraction, particularly when jet flows were directed along a sidewall. Obviously, there are a range of scale dependent issues [70], given the limitations to two juvenile fish species and extrapolation of experimental results to field applicability. Future research should test whether other fish species and fish sizes at different life stages and in field

settings behave similarly. Expanding beyond slotted entrance designs, to other opening geometries [37] and their effects on hydrodynamics and fish attraction behaviour are also important.

6 Conclusion

Investigations of the relationships between fish behaviour at slotted fishway entrances and hydrodynamics are rare. Interactions between flow hydrodynamics and fish behaviour of two Australian fish species, one coastal and the other inland, were investigated. There were complex interactions but clearly fish were attracted to flow. Importantly, there were interesting ramifications for improving the effectiveness of slotted fishway entrances. Different attraction flow hydrodynamic scenarios created improved fish attraction behaviour into fishways. Streamlined entrances performed better than plain entrances with fish capitalising on predictable zones of low turbulent kinetic energy for the former, as they were attracted to the entrances. Once fish were at the vicinity of the streamlined entrance (after approach), they frequently sought out the main attraction jet flow. Fish seem to be exploiting patterns of jet flows, swimming where swimming costs are probably minimised. There remains much to be learnt about the role of flow hydrodynamics in slotted and other fish entrances, which could further improve effectiveness of fishways and their ability to attract the range of species and different times of their life history.

Declarations

Compliance with Ethical Standards

Conflict of Interest: The authors declare that they have no conflict of interest.

Funding: The authors acknowledge financial support by the New South Wales Department of Primary Industries Recreational Fishing Trust (Project LF015), the Carthew Foundation, the Lord Mayor's Charitable Foundation and the Department of Education, Skills and Employment of the Australian Government (Regional Research Collaboration Program Shared Grant with Charles Sturt University). The first author was supported by a University of New South Wales Scientia PhD Scholarship.

Competing Interests: The authors have no competing interests to declare that are relevant to the content of this article.

Ethical approval: All experiments complied with Animal Care and Ethics requirements (ACEC approval 18/137A).

Informed consent: Informed consent was obtained from all individual participants included in the study.

Acknowledgement

All experiments complied with Animal Care and Ethics requirements (18/137A). We would like to warmly thank Adjunct Professor William Peirson and Adjunct Associate Professor John Harris for fruitful

discussions. We would also like to thank Reilly Cox for his help with fish keeping and Rob Jenkins and Larry Paice for their technical assistance. The authors acknowledge financial support by the New South Wales Department of Primary Industries Recreational Fishing Trust (Project LF015), the Carthew Foundation, the Lord Mayor's Charitable Foundation and the Department of Education, Skills and Employment of the Australian Government (Regional Research Collaboration Program Shared Grant with Charles Sturt University). The first author was supported by a University of New South Wales Scientia PhD Scholarship.

References

1. Wu H, Chen J, Xu J, Zeng G, Sang L, Liu Q, et al. Effects of dam construction on biodiversity: A review. J Clean Prod. 2019;221:480–9. https://doi.org/10.1016/j.jclepro.2019.03.001.
2. Cooke SJ, Paukert C, Hogan Z. Endangered river fish: factors hindering conservation and restoration. Endanger species Res. 2012;17(2):179–91.
3. Arthington AH, Dulvy NK, Gladstone W, Winfield IJ. Fish conservation in freshwater and marine realms: status, threats and management. Aquat Conservation: Mar Freshw Ecosyst. 2016;26(5):838–57. https://doi.org/10.1002/aqc.2712.
4. Katopodis C, Williams JG. The development of fish passage research in a historical context. Ecol Eng. 2012;48:8–18. https://doi.org/10.1016/j.ecoleng.2011.07.004.
5. Fuentes-Pérez JF, Eckert M, Tuhtan JA, Ferreira MT, Kruusmaa M, Branco P. Spatial preferences of Iberian barbel in a vertical slot fishway under variable hydrodynamic scenarios. Ecol Eng. 2018;125:131–42.
6. Ahmadi M, Kuriqi A, Nezhad HM, Ghaderi A, Mohammadi M. Innovative configuration of vertical slot fishway to enhance fish swimming conditions. J Hydrodynamics. 2022;34(5):917–33. 10.1007/s42241-022-0071-y.
7. Garavelli L, Linley TJ, Bellgraph BJ, Rhode BM, Janak JM, Colotelo AH. Evaluation of passage and sorting of adult Pacific salmonids through a novel fish passage technology. Fish Res. 2019;212:40–7.
8. Harris JH, Peirson WL, Mefford B, Kingsford RT, Felder S. Laboratory testing of an innovative tube fishway concept. J Ecohydraulics. 2020;5(1):84–93.
9. Peirson WL, Harris JH, Kingsford RT, Mao X, Felder S. Piping fish over dams. J Hydro-Environ Res. 2021;39:71–80. https://doi.org/10.1016/j.jher.2021.07.002.
10. Peirson WL, Harris JH, Suthers IM, Farzadkhoo M, Kingsford RT, Felder S. Impacts on fish transported in tube fishways. J Hydro-Environ Res. 2022;42:1–11. https://doi.org/10.1016/j.jher.2022.03.001.
11. Coombs S, Bak-Coleman J, Montgomery J. Rheotaxis revisited: a multi-behavioral and multisensory perspective on how fish orient to flow. J Exp Biol. 2020;223(23). 10.1242/jeb.223008.
12. Silva AT, Katopodis C, Santos JM, Ferreira MT, Pinheiro AN. Cyprinid swimming behaviour in response to turbulent flow. Ecol Eng. 2012;44:314–28.

https://doi.org/10.1016/j.ecoleng.2012.04.015.
13. Liao JC. A review of fish swimming mechanics and behaviour in altered flows. Philosophical Trans Royal Soc B: Biol Sci. 2007;362(1487):1973–93. 10.1098/rstb.2007.2082.
14. Tritico HM, Cotel AJ. The effects of turbulent eddies on the stability and critical swimming speed of creek chub (Semotilus atromaculatus). J Exp Biol. 2010;213(13):2284-93. doi: 10.1242/jeb.041806%J Journal of Experimental Biology.
15. Liao JC, Cotel A. Effects of Turbulence on Fish Swimming in Aquaculture. In: Palstra AP, Planas JV, editors. Swimming Physiology of Fish: Towards Using Exercise to Farm a Fit Fish in Sustainable Aquaculture. Berlin, Heidelberg: Springer Berlin Heidelberg; 2013. pp. 109–27.
16. Williams JG, Armstrong G, Katopodis C, Larinier M, Travade F. Thinking like a fish: a key ingredient for development of effective fish passage facilities at river obstructions. River Res Appl. 2012;28(4):407–17.
17. Foulds WL, Lucas MC. Extreme inefficiency of two conventional, technical fishways used by European river lamprey (Lampetra fluviatilis). Ecol Eng. 2013;58:423–33. https://doi.org/10.1016/j.ecoleng.2013.06.038.
18. Santos JM, Silva A, Katopodis C, Pinheiro P, Pinheiro A, Bochechas J, et al. Ecohydraulics of pool-type fishways: getting past the barriers. Ecol Eng. 2012;48:38–50.
19. Gisen DC, Schütz C, Weichert RB. Development of behavioral rules for upstream orientation of fish in confined space. PLoS ONE. 2022;17(2):e0263964.
20. Wang H, Chanson H, Kern P, Franklin C. Culvert hydrodynamics to enhance upstream fish passage: fish response to turbulence. Proceedings of the 20th Australasian Fluid Mechanics Conference, AFMC 2016: Australasian Fluid Mechanics Society; 2016. p. 682-1-4.
21. Silva AT, Lucas MC, Castro-Santos T, Katopodis C, Baumgartner LJ, Thiem JD, et al. The future of fish passage science, engineering, and practice. Fish Fish. 2018;19(2):340–62. https://doi.org/10.1111/faf.12258.
22. Mao X, Fu J-j, Tuo Y-c, An R-d, Li J. Influence of Structure on Hydraulic Characteristics of T Shape Fishway. J Hydrodynamics. 2012;24(5):684–91. 10.1016/S1001-6058(11)60292-8.
23. Cai L, Hou Y, Katopodis C, He D, Johnson D, Zhang P. Rheotaxis and swimming performance of Perch-barbel (Percocypris pingi, Tchang, 1930) and application to design of fishway entrances. Ecol Eng. 2019;132:102–8.
24. Chen M, An R, Li J, Li K, Li F. Identifying operation scenarios to optimize attraction flow near fishway entrances for endemic fishes on the Tibetan Plateau of China to match their swimming characteristics: A case study. Sci Total Environ. 2019;693:133615.
25. Mallen-Cooper M, Brand D. Non-salmonids in a salmonid fishway: what do 50 years of data tell us about past and future fish passage? Fisheries Manage. 2007;14(5):319–32.
26. Calles EO, Greenberg LA. Evaluation of nature-like fishways for re-establishing connectivity in fragmented salmonid populations in the River Emån. River Res Appl. 2005;21(9):951–60. https://doi.org/10.1002/rra.865.

27. Gisen DC, Weichert RB, Nestler JM. Optimizing attraction flow for upstream fish passage at a hydropower dam employing 3D Detached-Eddy Simulation. Ecol Eng. 2017;100:344–53.
28. Keefer ML, Peery CA, Lee SR, Daigle WR, Johnson EL, Moser ML. Behaviour of adult Pacific lamprey in near-field flow and fishway design experiments. Fish Manag Ecol. 2011;18(3):177–89. https://doi.org/10.1111/j.1365-2400.2010.00772.x.
29. FAO D, Rome. Fish passes: design, dimensions, and monitoring. Food and Agriculture Organization of the United Nations in arrangement with Deutscher Verband für Wasserwirtschaft und Kulturbau e.V. (DVWK); 2002.
30. Tang J, Gao C, Chen M, An R-d, Bai R-n. JIANG Y-c. Study on influence of different flow patterns on fish attracting effect at fish way entrance. Hongshui River. 2013;32(1):34–9.
31. Amaral SD, Branco P, da Silva AT, Katopodis C, Viseu T, Ferreira MT, et al. Upstream passage of potamodromous cyprinids over small weirs: the influence of key-hydraulic parameters. J Ecohydraulics. 2016;1(1–2):79–89. 10.1080/24705357.2016.1237265.
32. Mu X, Zhen W, Li X, Cao P, Gong L, Xu F. A study of the impact of different flow velocities and light colors at the entrance of a fish collection system on the upstream swimming behavior of juvenile grass carp. Water. 2019;11(2):322.
33. Farzadkhoo M, Kingsford RT, Suthers IM, Geelan-Small P, Harris JH, Peirson W, et al. Attracting juvenile fish into Tube Fishways – roles of transfer chamber diameter and flow velocity. Ecol Eng. 2022;176:106544. https://doi.org/10.1016/j.ecoleng.2022.106544.
34. Farzadkhoo M, Kingsford RT, Suthers IM, Harris JH, Peirson W, Felder S. Australian Native Fish Attracted by Jet Flows into Tube Fishways. 39th IAHR World Congress. Granada, Spain2022.
35. Bretón F, Baki ABM, Link O, Zhu DZ, Rajaratnam N. Flow in nature-like fishway and its relation to fish behaviour. Can J Civ Eng. 2013;40(6):567–73. 10.1139/cjce-2012-0311.
36. Rodi W. Turbulence Models and Their Application in Hydraulics. London: Routledge; 2000.
37. Guiny E, Ervine DA, Armstrong JD. Hydraulic and biological aspects of fish passes for Atlantic salmon. J Hydraul Eng. 2005;131(7):542–53.
38. Liu M, Rajaratnam N, Zhu DZ. Mean flow and turbulence structure in vertical slot fishways. J Hydraul Eng. 2006;132(8):765–77.
39. Morrison RR, Hotchkiss RH, Stone M, Thurman D, Horner-Devine AR. Turbulence characteristics of flow in a spiral corrugated culvert fitted with baffles and implications for fish passage. Ecol Eng. 2009;35(3):381–92. https://doi.org/10.1016/j.ecoleng.2008.10.012.
40. Silva AT, Santos JM, Ferreira MT, Pinheiro AN, Katopodis C. Effects of water velocity and turbulence on the behaviour of Iberian barbel (Luciobarbus bocagei, Steindachner 1864) in an experimental pool-type fishway. River Res Appl. 2011;27(3):360–73. https://doi.org/10.1002/rra.1363.
41. Syms JC, Kirk MA, Caudill CC, Tonina D. A biologically based measure of turbulence intensity for predicting fish passage behaviours.Journal of Ecohydraulics. 2021:1–13. doi: 10.1080/24705357.2020.1856007.

42. Li G, Sun S, Liu H, Zheng T. Schizothorax prenanti swimming behavior in response to different flow patterns in vertical slot fishways with different slot positions. Sci Total Environ. 2021;754:142142. https://doi.org/10.1016/j.scitotenv.2020.142142.
43. Tan J, Tan H, Goerig E, Ke S, Huang H, Liu Z, et al. Optimization of fishway attraction flow based on endemic fish swimming performance and hydraulics. Ecol Eng. 2021;170:106332. https://doi.org/10.1016/j.ecoleng.2021.106332.
44. White FM. Fluid mechanics. 8th edition ed. New York: Tata McGraw-Hill Education; 2016.
45. Goring DG, Nikora VI. Despiking acoustic Doppler velocimeter data. J Hydraul Eng. 2002;128(1):117–26.
46. Wahl TL. Discussion of “Despiking acoustic doppler velocimeter data” by Derek G. Goring and Vladimir I. Nikora. J Hydraul Eng. 2003;129(6):484–7.
47. Lenth R. Estimated Marginal Means, aka Least-Squares Means. R package version 1.5. 4. 2021.
48. Brown CW, Hanson R. Tracker Video Analysis and Modelling Js (Beta), Version 5.9. 2020.
49. Demissie M. Diffusion of three-dimensional slot jets with deep and shallow submergence. Ann Arbor: University of Illinois at Urbana-Champaign; 1980. p. 211.
50. Mahl L, Heneka P, Henning M, Weichert RB. Numerical Study of Three-Dimensional Surface Jets Emerging from a Fishway Entrance Slot. Water. 2021;13(8):1079.
51. Marriner BA, Baki AB, Zhu DZ, Cooke SJ, Katopodis C. The hydraulics of a vertical slot fishway: A case study on the multi-species Vianney-Legendre fishway in Quebec, Canada. Ecol Eng. 2016;90:190–202.
52. Bourque C, Newman B. Reattachment of a two-dimensional, incompressible jet to an adjacent flat plate. Aeronaut Q. 1960;11(3):201–32.
53. Miozzi M, Lalli F, Romano GP. Experimental investigation of a free-surface turbulent jet with Coanda effect. Exp Fluids. 2010;49(1):341–53. 10.1007/s00348-010-0885-1.
54. Dumas A, Subhash M, Trancossi M, Marques JP. The influence of surface temperature on Coanda effect. Energy Procedia. 2014;45:626–34.
55. Webb PW. The effect of solid and porous channel walls on steady swimming of steelhead trout Oncorhynchus mykiss. J Exp Biol. 1993;178(1):97–108.
56. Plaut I, Part A, Molecular. Integr Physiol. 2001;131(1):41–50. https://doi.org/10.1016/S1095-6433(01)00462-7.
57. Johnson K, Wait LE, Monk SK, Rader R, Hotchkiss RH, Belk MC. Effects of substrate on movement patterns and behavior of stream fish through culverts: An experimental approach. Sustainability. 2019;11(2):470.
58. Watson JR, Goodrich HR, Cramp RL, Gordos MA, Franklin CE. Utilising the boundary layer to help restore the connectivity of fish habitats and populations. Ecol Eng. 2018;122:286–94.
59. Wang R-W, David L, Larinier M. Contribution of experimental fluid mechanics to the design of vertical slot fish passes.Knowledge Management of Aquatic Ecosystems. 2010(396):02.

60. Liao L, Chen M, An R, Li J, Tang X, Yan Z. Identifying three-dimensional swimming corridors for fish to match their swimming characteristics under different hydropower plant operations: Optimization of entrance location for fish-passing facilities. Sci Total Environ. 2022;822:153599. https://doi.org/10.1016/j.scitotenv.2022.153599.
61. Goettel MT, Atkinson JF, Bennett SJ. Behavior of western blacknose dace in a turbulence modified flow field. Ecol Eng. 2015;74:230–40. https://doi.org/10.1016/j.ecoleng.2014.10.012.
62. Dabiri JO. How fish feel the flow. Nature. 2017;547(7664):406–7. 10.1038/nature23096.
63. Goerig E, Castro-Santos T. Is motivation important to brook trout passage through culverts? Can J Fish Aquat Sci. 2017;74(6):885–93.
64. Mulligan K, Haro A, Towler B, Sojkowski B, Noreika J. Fishway Entrance Gate Experiments With Adult American Shad. Water Resour Res. 2019;55(12):10839–55.
65. Baki ABM, Zhu DZ, Rajaratnam N. Turbulence characteristics in a rock-ramp-type fish pass. J Hydraul Eng. 2015;141(2):04014075.
66. Gao Z, Andersson HI, Dai H, Jiang F, Zhao L. A new Eulerian–Lagrangian agent method to model fish paths in a vertical slot fishway. Ecol Eng. 2016;88:217–25.
67. Kirk MA, Caudill CC, Tonina D, Syms JC. Effects of water velocity, turbulence and obstacle length on the swimming capabilities of adult Pacific lamprey. Fish Manag Ecol. 2016;23(5):356–66. https://doi.org/10.1111/fme.12179.
68. Romão F, Quaresma AL, Branco P, Santos JM, Amaral S, Ferreira MT, et al. Passage performance of two cyprinids with different ecological traits in a fishway with distinct vertical slot configurations. Ecol Eng. 2017;105:180–8.
69. An R-d, Li J, Yi W-m, Mao X. Hydraulics and swimming behavior of schizothorax prenanti in vertical slot fishways. J Hydrodynamics. 2019;31(1):169–76. 10.1007/s42241-019-0009-1.
70. Wilkes MA, Maddock I, Visser F, Acreman MC. Incorporating Hydrodynamics into Ecohydraulics: The Role of Turbulence in the Swimming Performance and Habitat Selection of Stream-Dwelling Fish.Ecohydraulics. 2013. p.7–30.
71. Mallen-Cooper M, Brand DA. Non-salmonids in a salmonid fishway: what do 50 years of data tell us about past and future fish passage? Fish Manag Ecol. 2007;14(5):319–32. https://doi.org/10.1111/j.1365-2400.2007.00557.x.
72. Bunt C, Castro-Santos T, Haro A. Performance of fish passage structures at upstream barriers to migration. River Res Appl. 2012;28(4):457–78.
73. Wang R-W, David L, Larinier M. Contribution of experimental fluid mechanics to the design of vertical slot fish passes. Knowl Manage Aquat Ecosyst. 2010;396:02.
74. Marriner BA, Baki ABM, Zhu DZ, Thiem JD, Cooke SJ, Katopodis C. Field and numerical assessment of turning pool hydraulics in a vertical slot fishway. Ecol Eng. 2014;63:88–101. https://doi.org/10.1016/j.ecoleng.2013.12.010.
75. Rajaratnam N. Turbulent jets. Elsevier; 1976.

Figures

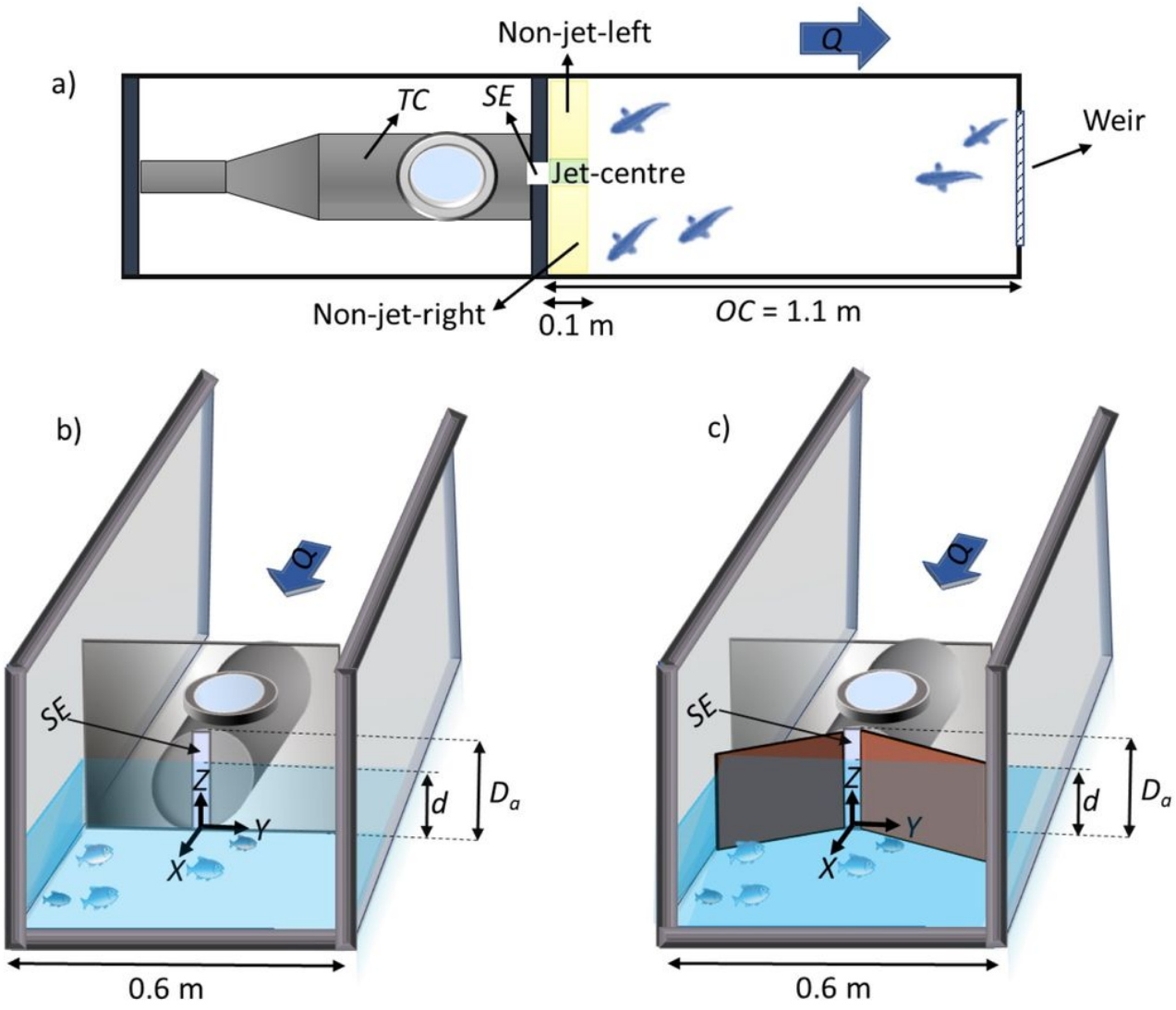

Figure 1

Sketch of the experimental setup for testing relationships between fish behaviour and hydrodynamics of slotted fishway entrances, showing: a) top view of the setup with the transfer chamber (*TC*), slotted entrance (*SE*) and observation channel (*OC)* for the plain slotted entrance design, with the arrow showing the direction of flow and the attraction zone adjacent to the slotted entrance (yellow and green shadings, defining the pre-entry location) segmented into jet (centre) and non-jet regions (left and right) and the same experimental setup but for the two designs of b) plain entrance and c) streamlined entrance, with the coordinate system defined at the centre bottom of the slotted entrance

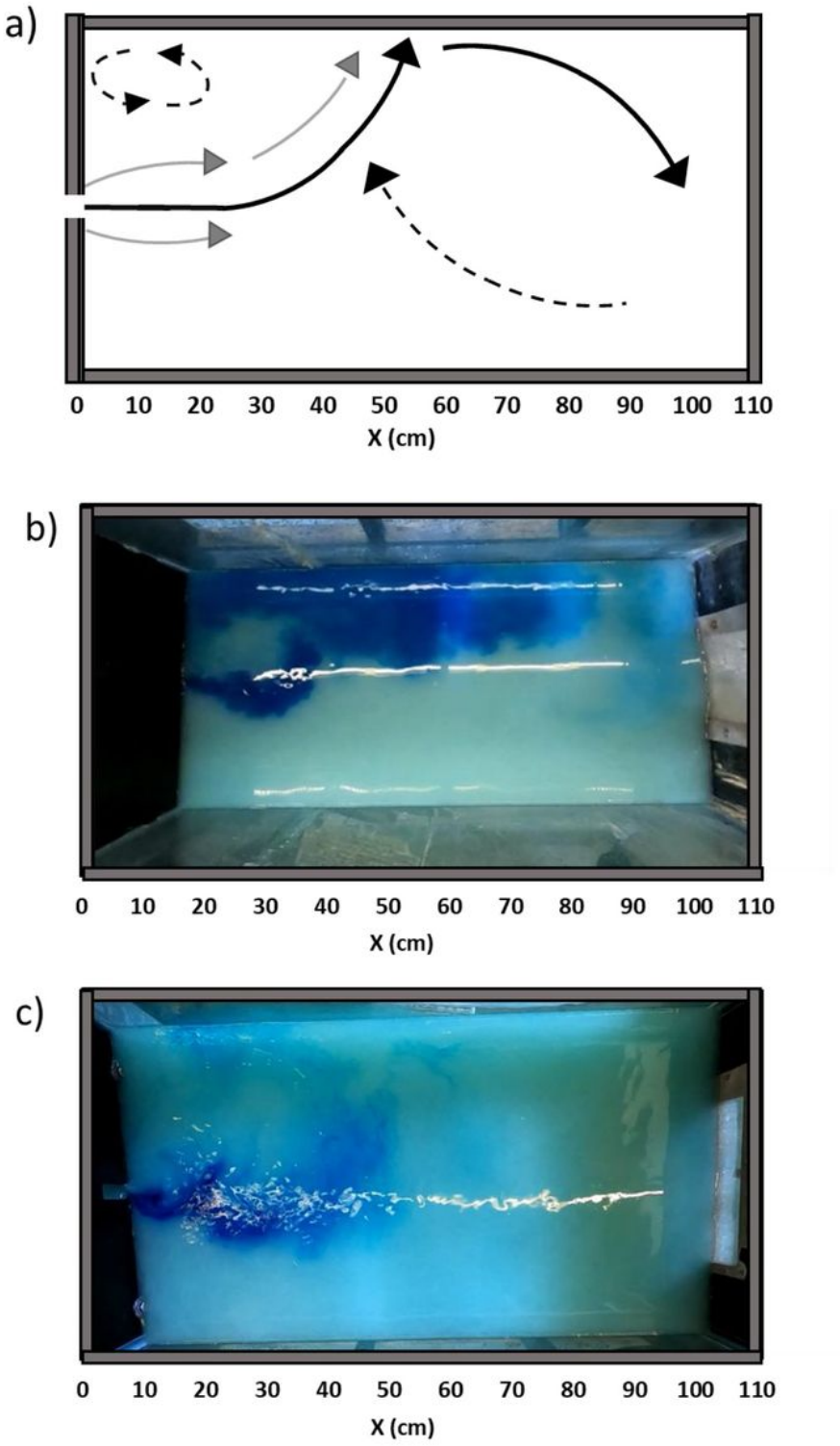

Figure 2

Flow patterns of jet flow downstream of a plain entrance: a) conceptional jet flow patterns, with main jet trajectories (solid arrows, black showing main direction and grey showing dispersed/reduced flow) and recirculation motions (dashed arrows); b) dye (dark blue) trajectories for d = 0.08 m, V_a= 0.15 m/s and c) d = 0.32 m, V_a = 0.15 m/s

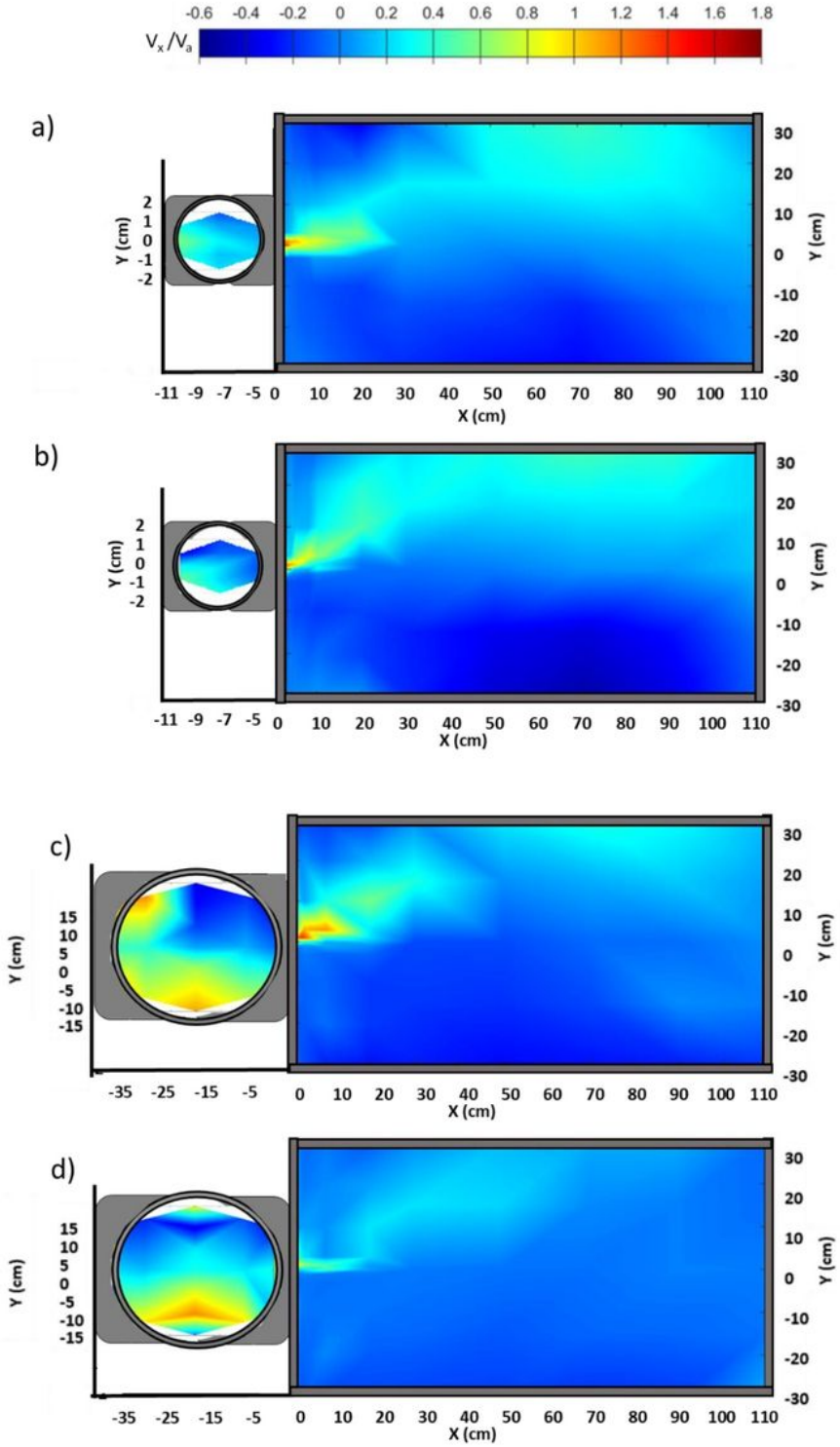

Figure 3

Normalised streamwise velocities upstream and downstream of a plain slotted entrance at Z = 0.3 *d* for: a) *d* = 0.08 m, V_a = 0.15 m/s; b) *d* = 0.08 m, V_a = 0.5 m/s; c) *d* = 0.32 m, V_a = 0.15; and d) *d* = 0.32 m, V_a = 0.5 m/s

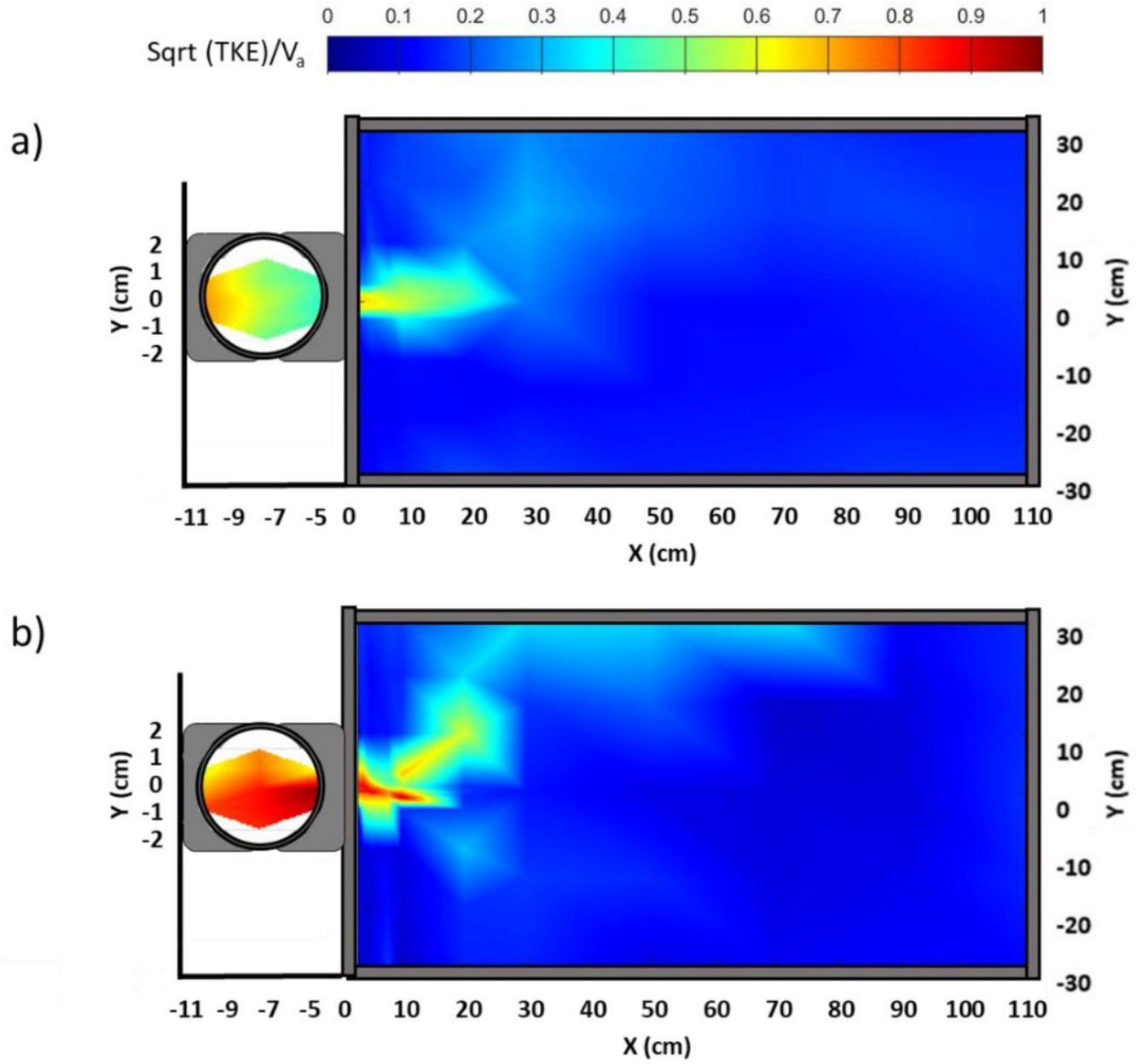

Figure 4

Normalised turbulent kinetic energy observations for a plain slotted entrance at $Z = 0.3\ d$ for $d = 0.08$ m; a) $V_a = 0.15$ m/s; b) $V_a = 0.5$ m/s

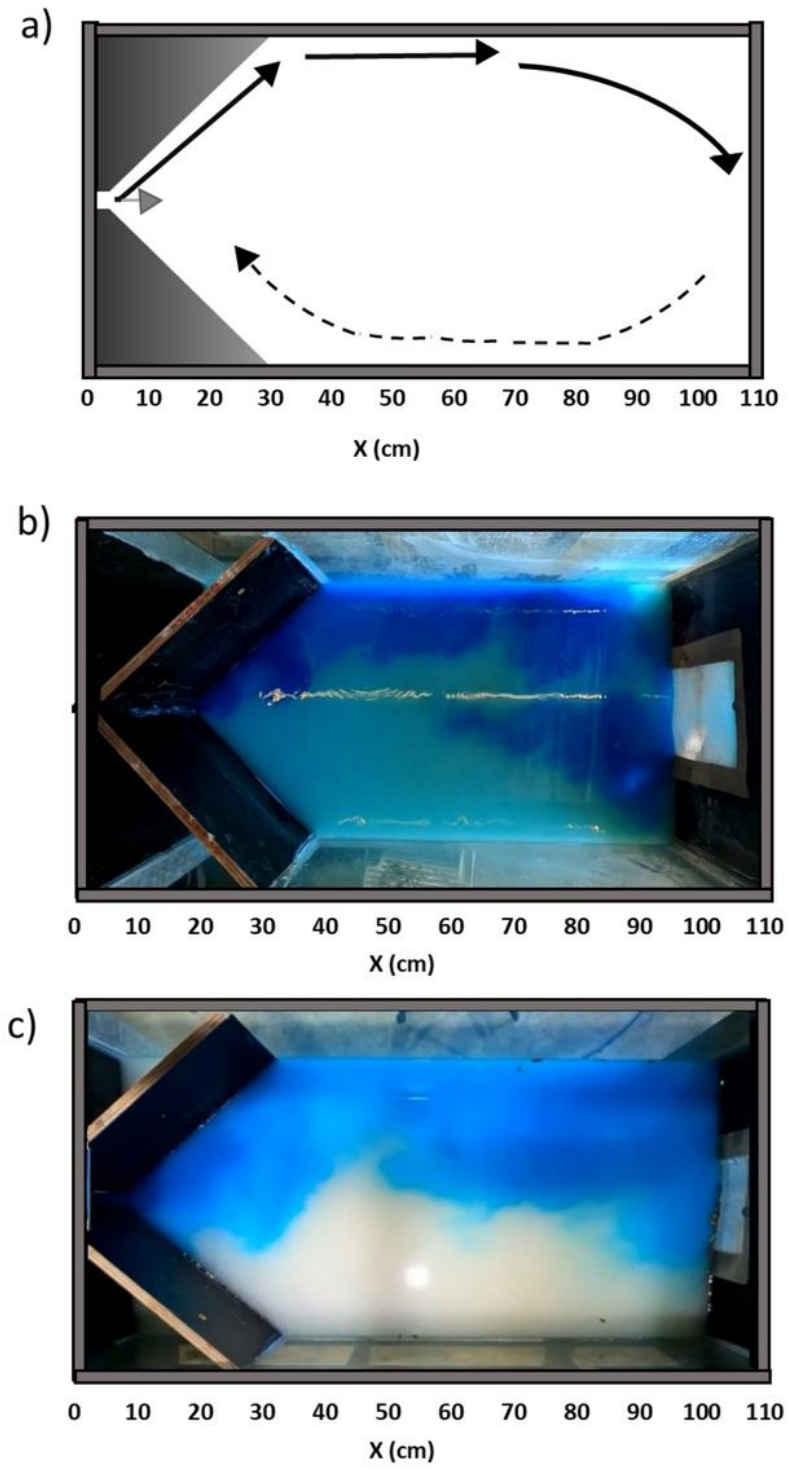

Figure 5

Flow patterns of attraction flow for a streamlined entrance: a) conceptional jet flow patterns with the main jet trajectory (solid arrows) and recirculation motions (dashed arrows); b) dye (dark blue) trajectories for d = 0.08 m, V_a= 0.15 m/s; and c) d = 0.18 m, V_a = 0.15 m/s

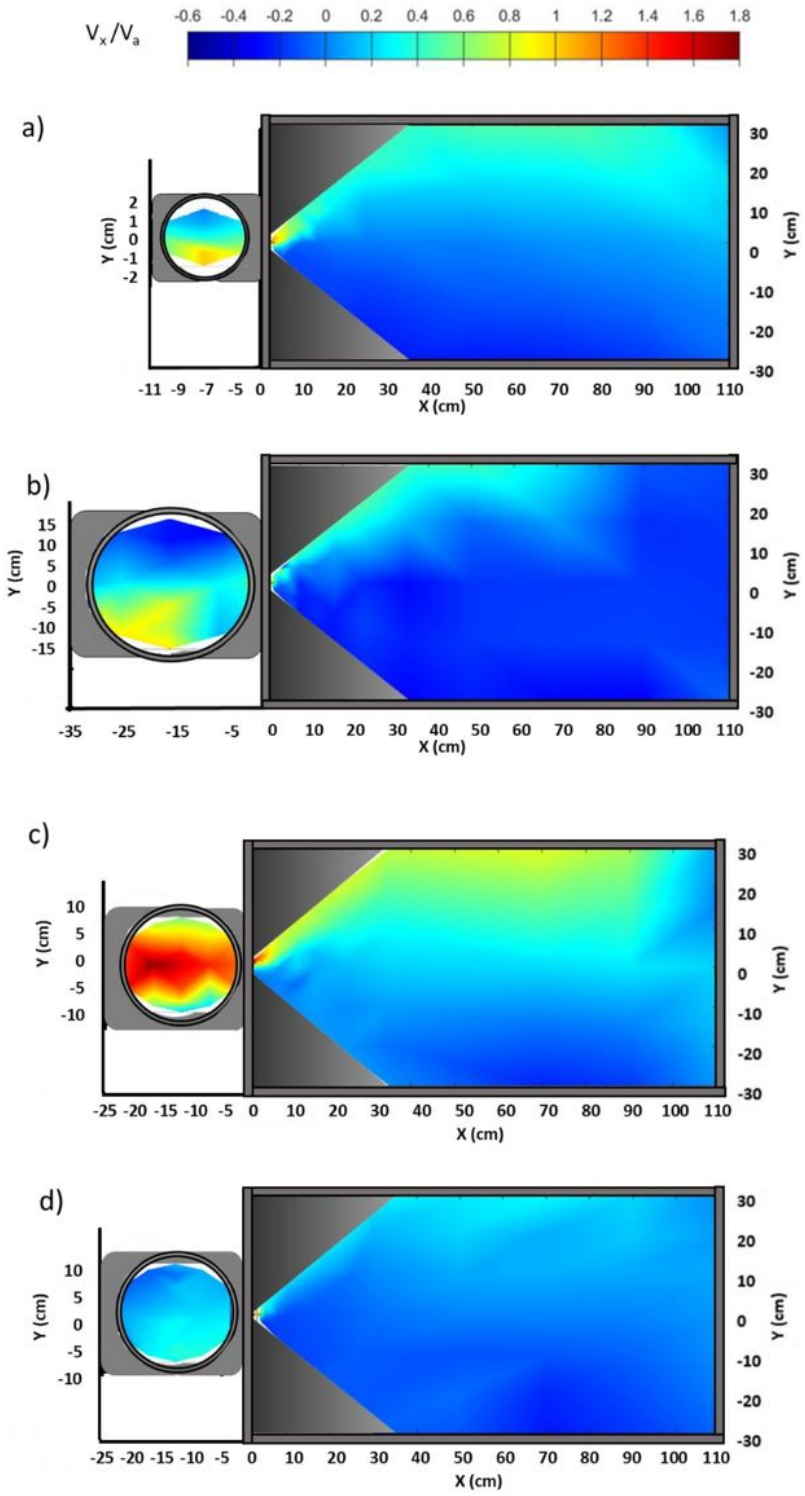

Figure 6

Normalised streamwise velocities upstream and downstream of a streamlined slotted entrance at $Z = 0.3$ d for a) $d = 0.08$ m, $V_a = 0.15$ m/s; b) $d = 0.32$ m, $V_a = 0.15$ m/s, and at $Z = 0.1$ d for c) $d = 0.18$ m and $V_a = 0.15$ m/s; d) $d = 0.18$ m and $V_a = 0.15$ m/s

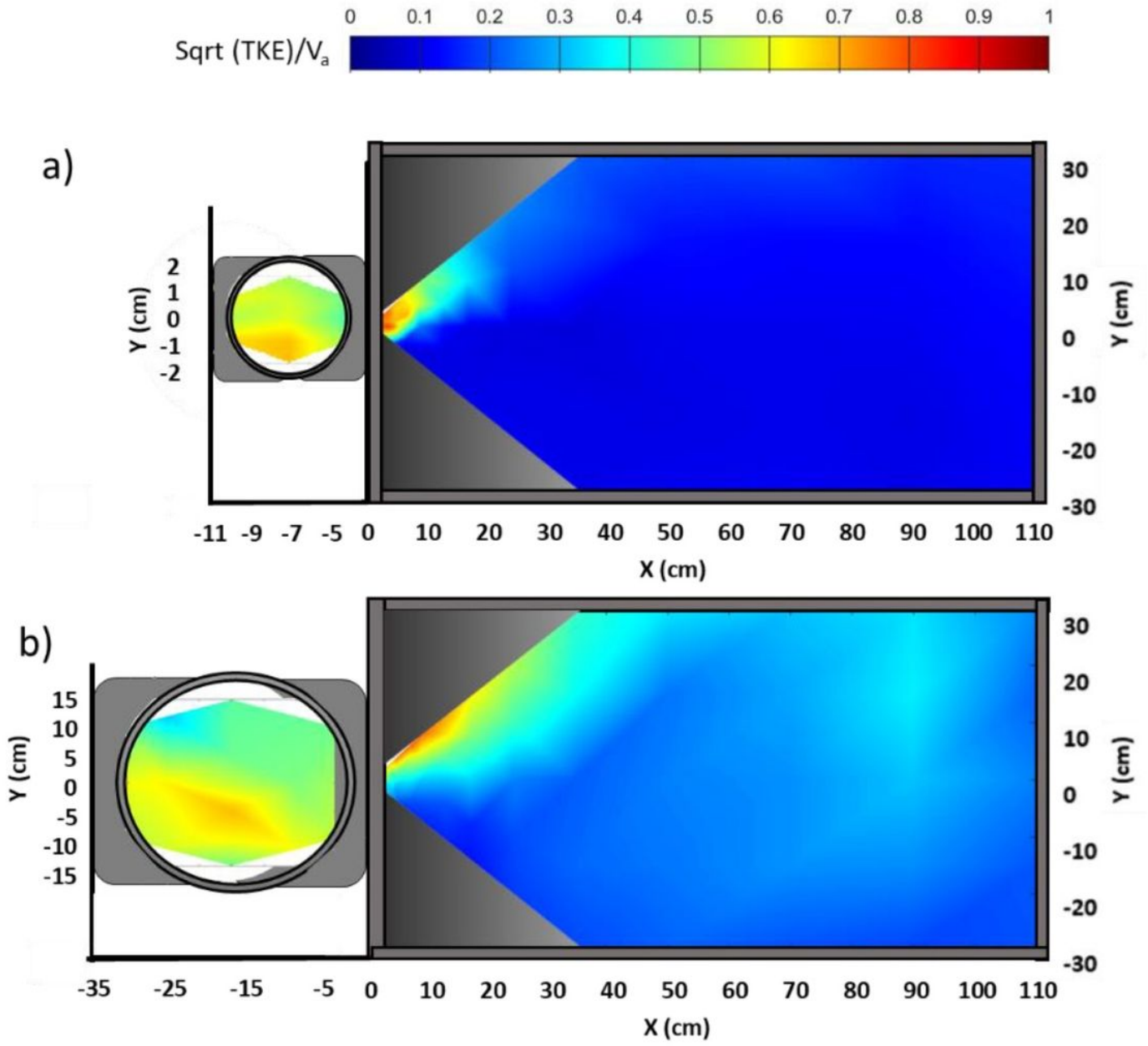

Figure 7

Normalised turbulent kinetic energy for a streamlined entrance at $Z = 0.3\ d$ for; a) $d = 0.08$ m, $V_a = 0.15$ m/s; b) $d = 0.32$ m, $V_a = 0.15$ m/s

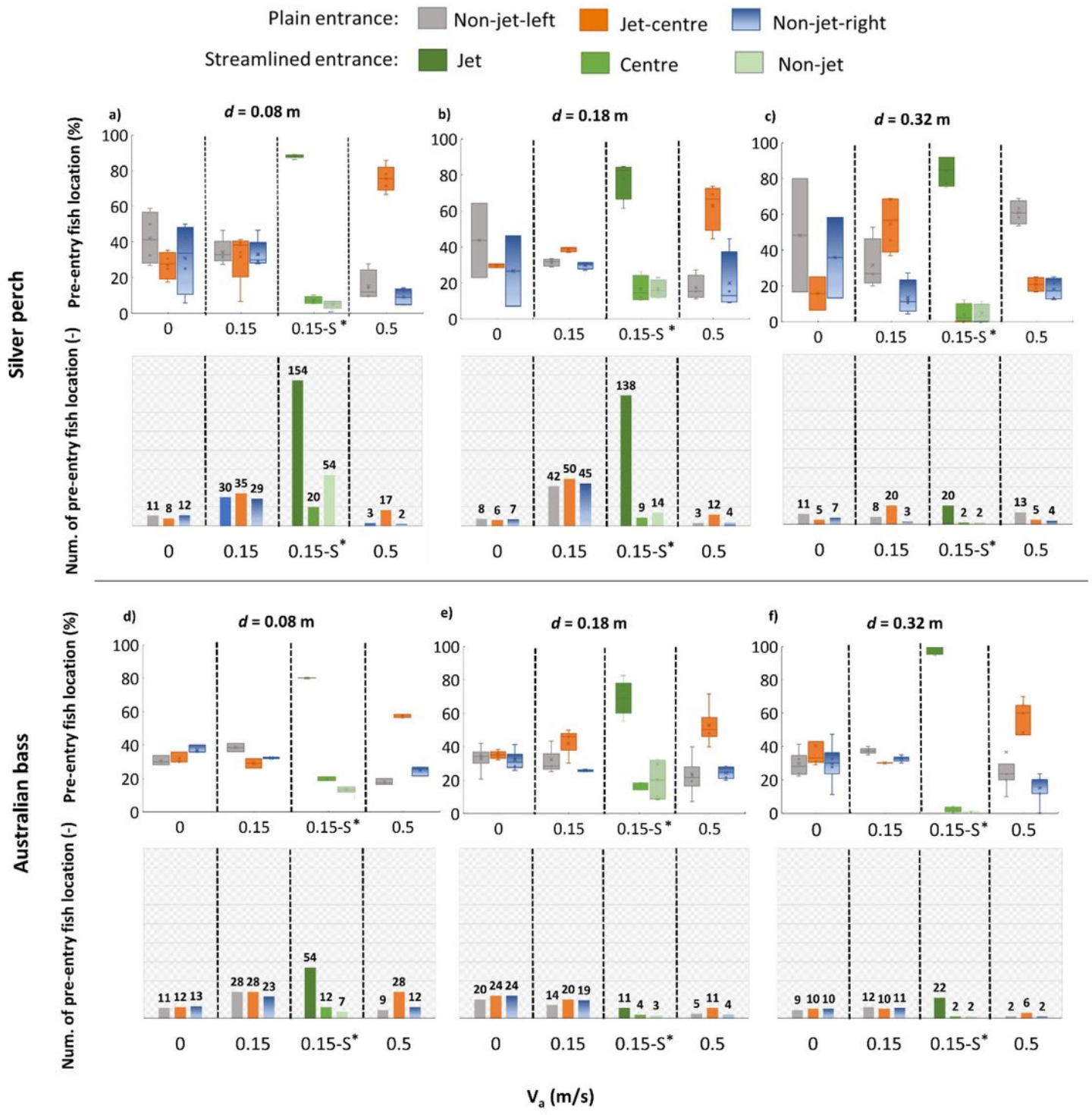

Figure 8

Pre-entry locations for repetitive entries of silver perch (a-c) and Australian bass (d-f) for variation in attraction velocities (V_a) and water depths (d) in relation to directions of the attraction jet for plain (grey, orange, and blue colours) and *streamlined (green colours) entrances

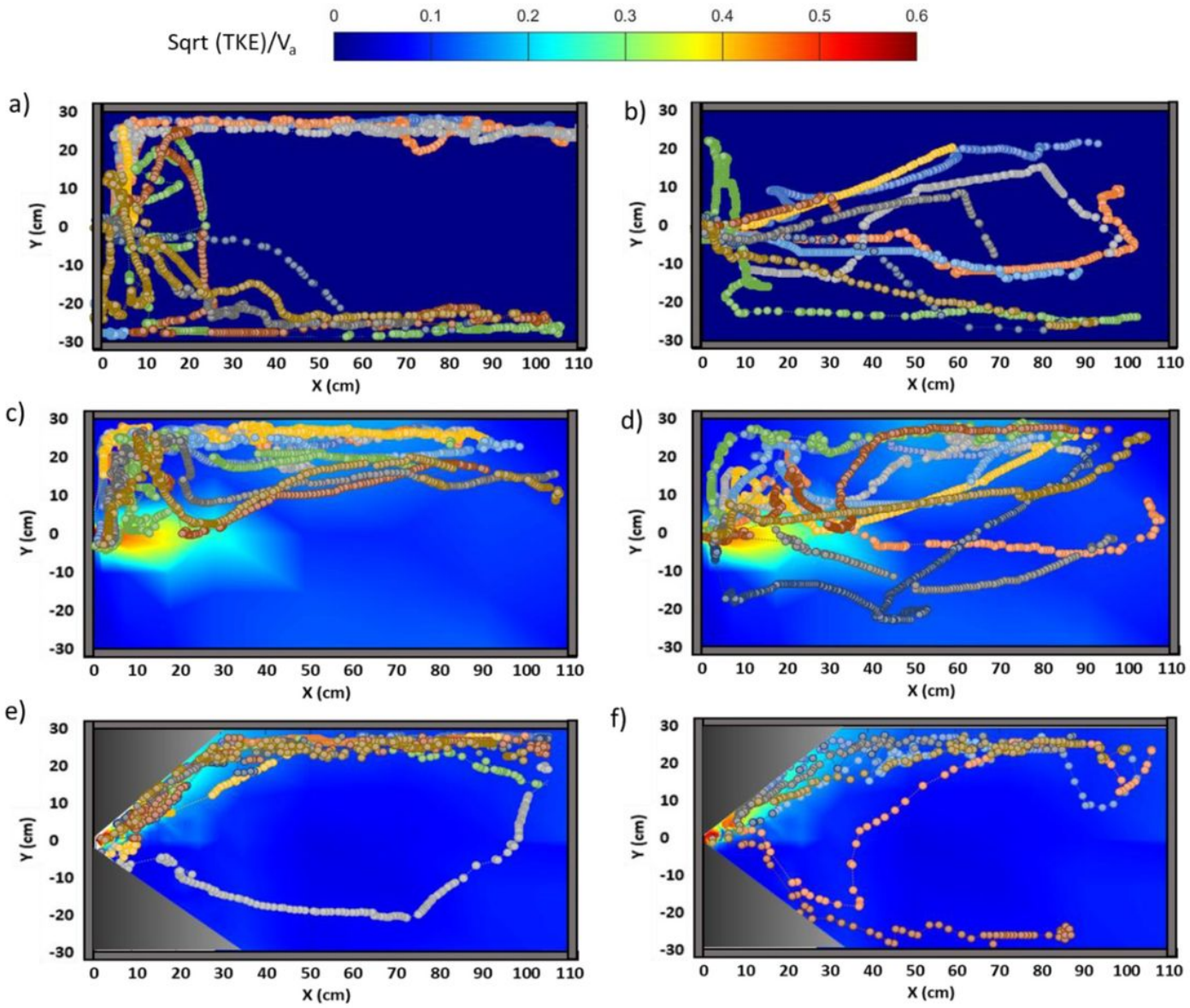

Figure 9

Fish movement trajectories (right to left), with flow (left to right), projected onto $\sqrt{TKE} / V_a$ for selected trials of d = 0.18 m at Z = 0.3 d for silver perch a) V_a = 0 m/s (plain entrance); c) V_a = 0.15 m/s (plain entrance); and e) V_a = 0.15 m/s (streamlined entrance), and Australian bass b) V_a = 0 m/s (plain entrance); d) V_a = 0.15 m/s (plain entrance); and f) V_a = 0.15 m/s (streamlined entrance)

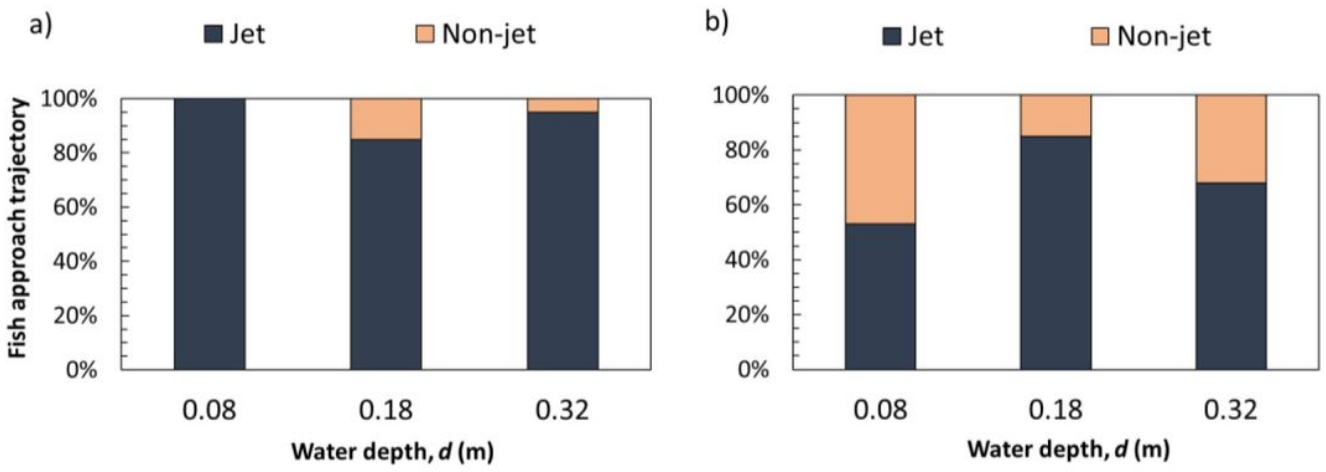

Figure 10

First fish entry trajectories (percentages) for the streamlined entrance in relation to jet and non-jet areas for various depths (d) and V_a = 0.15 m/s for: a) silver perch; b) Australia bass

Supplementary Files

This is a list of supplementary files associated with this preprint. Click to download.

- Appendices.docx
- supplementaryMaterialMF.docx